Acta Cryst. (1998). B**54**, 790–797

Isotope Effect in TlH_2PO_4 and TlD_2PO_4

S. Ríos,[a]*† W. Paulus,[a,b] A. Cousson,[a] M. Quilichini[a] and G. Heger[b]

[a]*Laboratoire Léon Brillouin, CEA-CNRS Saclay, 91191 Gif-sur-Yvette CEDEX, France, and* [b]*RWTH Aachen, Institut für Kristallographie, Jägerstrasse 17-19, D-52056 Aachen, Germany. E-mail: rios@esc.cam.ac.uk.*

(*Received 14 November 1997; accepted 6 April 1998*)

Abstract

The crystal structure of the antiferroelectric phase of TlD_2PO_4, deuterated thallium dihydrogenphosphate, has been determined from single-crystal neutron diffraction data collected at room temperature. The para-antiferroelectric transition (T_c^d = 353 K) of TlD_2PO_4 is analysed from a structural point of view and compared with the phase transition of TlH_2PO_4 at T_I = 357 K, already characterized. The distinct phase sequences observed in the two compounds when decreasing temperature from that of the high-temperature prototype phase (prototype phase/room-temperature phase/low-temperature phase) are discussed and associated with the different ordering of the two crystallographically inequivalent H (D) atoms existing in the prototype phase.

1. Introduction

TlH_2PO_4 and its deuterated form TlD_2PO_4 belong to the large family of hydrogen-bonded (anti)ferroelectric materials of the KH_2PO_4 (KDP) type. Similar to the other compounds of the $A(H,D)_2PO_4$ family (with A = K^+, Rb^+, Cs^+ and NH_4^+), TlH_2PO_4 and TlD_2PO_4 show a large isotope effect in their Curie temperatures: T_c^h = 230 K and T_c^d = 353 K, where the upper indices h and d indicate the protonated and deuterated compounds, respectively. It is well known from dielectric and calorimetric measurements (Bousquet *et al.*, 1978; Matsuo & Suga, 1977; Hanazawa *et al.*, 1991) that these two compounds exhibit two phase transitions: for TlH_2PO_4 at T_I = 357 K and T_c^h = 230 K, and for TlD_2PO_4 at T_c^d = 353 K and T_d = 127 K. It has been assumed from X-ray measurements (Nelmes, 1981) that the two paraelectric phases (357 > T > 230 K in TlH_2PO_4 and T > 353 K in TlD_2PO_4) are isomorphous, the transitions at 230 and 353 K, respectively, being structurally equivalent. Nevertheless, recent single-crystal neutron diffraction experiments at 373 K and room temperature on both TlH_2PO_4 and the highly deuterated TlD_2PO_4 have demonstrated that the phase sequences are not at all equivalent in the two cases and that the degree of deuteration seems to play an important role in the structures of these two compounds.

Measurements at 373 K revealed the high-temperature phases, *i.e.* $T > T_I$ for TlH_2PO_4 and $T > T_c^d$ for TlD_2PO_4 (Ríos *et al.*, 1995, hereafter referred to as R95), to be isostructural. We shall hereafter denote this phase the *prototype phase*. This phase has orthorhombic symmetry with the space group *Pbcn* (D_{2h}^{14}). The paraelectric phase of TlD_2PO_4 is not, therefore, isomorphous with the paraelectric phase of TlH_2PO_4. This latter phase in TlH_2PO_4 is known to have monoclinic symmetry, as reported by Nelmes & Choudhary (1981). Furthermore, and despite the fact that both compounds are isostructural at high temperatures, they undergo, when cooling from the prototype-phase temperature, two radically different phase transitions. Concerning TlH_2PO_4, the transition at T_I is known to be ferroelastic. The softening of the C_{44} elastic constant, by means of ultrasonic measurements (Hanazawa *et al.*, 1991), as well as the instability of the corresponding transverse acoustic mode by Brillouin scattering (Arai *et al.*, 1990) have already been observed. However, up to now there has been no evidence for the existence of a possible soft optic mode at T_I. Thus, it has not yet been established whether the instability yields a proper ferroelastic phase or if an optic mode is also involved in the mechanism, leading to a pseudo-proper ferroelastic phase. The structure of the ferroelastic room-temperature monoclinic phase has already been studied, first with X-rays (Oddon *et al.*, 1979) and later with neutron diffraction (Nelmes & Choudhary, 1981). At T_I the symmetry changes from the orthorhombic space group *Pbcn* to the monoclinic $P2_1/b11$,‡ with the a axis of the prototype phase being the monoclinic axis. The number of formula units per unit cell is conserved and the cell parameters do not differ significantly from those of the prototype phase, apart from the fact that a spontaneous shear strain, e_4, appears at the transition [room-temperature lattice parameters are a = 4.525 (3), b = 14.33 (1), c = 6.526 (6) Å and α = 91.76 (7)°, which agree with those obtained by Nelmes & Choudhary (1981)].

† Current address: Department of Earth Sciences, University of Cambridge, Downing Street, Cambridge CB2 3EQ, England.

‡ $P2_1/b11$ is a non-standard setting of the space group $P12_1/c1$. Even though it does not correspond to that used by Nelmes & Choudhary (1981), we prefer to keep this setting in order to compare the prototype phase and TlD_2PO_4 in a more comprehensive way.

ISSN 0108-7681

Table 1. *Diagonal components of the* **T** *translational (Å^2) and* **L** *librational (deg^2) tensors of the rigid-body motion analysis of the PO_4 groups of TlH_2PO_4 and TlD_2PO_4 at 373 K, from the data reported in R95*

The parameters are referenced to the Cartesian crystal frame. wR, the agreement factor, is defined as $[\sum w(\Delta U^{ij})^2 / \sum w(U^{ij})^2]^{1/2}$, with the weights w taken as inversely proportional to the variance of U^{ij}. n_o and n_r are the number of independent observations and refined rigid-body parameters, respectively, used in the **TLS** analysis.

	L_{11}	L_{22}	L_{33}	T_{11}	T_{22}	T_{33}	wR	n_o	n_r
TlH_2PO_4	118 (10)	30 (10)	25 (9)	0.032 (2)	0.035 (2)	0.032 (2)	0.028	18	12
TlD_2PO_4	112 (18)	53 (18)	25 (17)	0.031 (4)	0.033 (4)	0.032 (4)	0.060	18	12

For the deuterated compound TlD_2PO_4, the situation was rather ambiguous regarding the symmetry and the structure of the room-temperature phase. From the double hysteresis loops observed along the *a* axis (Yasuda, Fujimoto & Asano, 1980) the antiferroelectric nature of this phase was known; the crystal symmetry, however, was not clearly established. Several X-ray studies had already been carried out (Oddon *et al.*, 1976; Nelmes, 1981; Narasaiah *et al.*, 1986), arriving at contradictory conclusions concerning the unit-cell dimensions and the space-group symmetry of the room-temperature phase of TlD_2PO_4.

The purpose of this paper is therefore, first, to report our room-temperature neutron diffraction results for the highly deuterated TlD_2PO_4 and, second, to discuss the different phase transition sequences of TlH_2PO_4 and TlD_2PO_4 from a structural point of view. The paper is thus divided as follows: in §2, the most relevant aspects of the prototype phase are briefly recalled; in §3 and §4, the experimental details of the data collection and refinement of the room-temperature phase of TlD_2PO_4 are reported; in §5, the main features of this structure are described; finally, §6 is devoted to the comparison of TlH_2PO_4 and TlD_2PO_4.

2. Prototype phase (R95)

The high-temperature structure of both compounds is characterized by the existence of two crystallographically inequivalent H (D) atoms, hereafter numbered H1 (D1) and H2 (D2), respectively (see Fig. 1). The first type of H (D) atom links PO_4 groups in zigzag-like chains parallel to the *c* axis, while the second type links these chains along the *a* axis. In this way, hydrogen bonds form a two-dimensional network parallel to the *ac* plane. The structure is thus composed of independent layers packed perpendicular to the *b* axis and linked together by Coulombic interactions with Tl^+ ions. In this phase both types of H (D) atoms are believed to be disordered in a double well potential along the hydrogen bond, as already observed in other homologous compounds [*e.g.* KDP and its deuterated form DKDP (Nelmes *et al.*, 1982)]. This hypothesis is reinforced by the large anisotropy observed in their mean-square displacement parameters along this direction. Attempts to determine the distance between the two off-centre positions (commonly known as the δ distance) were not successful owing to the lack of resolution (see R95). In these two compounds it seems rather difficult to measure with accuracy the δ distance due to the high temperatures involved and the resulting thermal vibration. As also reported in R95, deuteration is accompanied by an increase of 2% of the oxygen–hydrogen–oxygen (O···O) bond distance, which is comparable to the increase observed for KDP and DKDP (Tun *et al.*, 1988).

Inspection of the atomic mean-square displacement ellipsoids of the O atoms (R95) makes apparent the existence of a rotational and (or) translational motion of the PO_4 rigid-body group. We tried to obtain quantitative evidence of these motions by fitting the U^{ij} parameters of the atoms of the PO_4 group to an overall rigid-body motion **TLS** (Schomaker & Trueblood, 1968). The values obtained for the diagonal components of the translational **T** and rotational **L** tensors are given in Table 1: the major component of the motion at 373 K has a librational character of amplitude $\sim 10^\circ$ involving a rotation around the *a* axis. It should be stressed that the results of the rigid-bond test (Hirshfeld, 1976) in the case of TlH_2PO_4 are quite good. The r.m.s. of the difference of the mean-square displacement amplitude (m.s.d.a.) for the bonded pairs of atoms (P—O) in the direction of the bond is 31×10^{-4} Å^2, with an estimated $\sigma \simeq 21 \times 10^{-4}$ Å^2, which should be compared with the r.m.s. for non-bonded pairs (O···O) of 16×10^{-4} Å^2, no larger than for the bonded pairs. However, in the case of

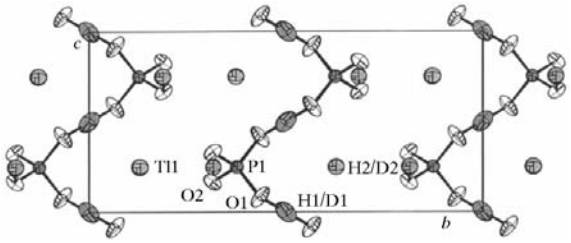

Fig. 1. Projection of the structure of the prototype phase of TlH_2PO_4 and TlD_2PO_4 along the [100] direction. The displacement ellipsoids enclose 30% probability. As the two off-centre positions of H (D) atoms could not be precisely determined, these atoms have been situated at the centre of O···O.

TlD_2PO_4 the rigid-body approximation is less accurate (the r.m.s. values are 12×10^{-4} and 58×10^{-4} Å^2 for P—O and O···O pairs, respectively), as can be seen from the larger agreement factor of the fit. This result is probably related to the fact that at the same temperature, PO_4 groups in TlD_2PO_4 are internally more distorted than in TlH_2PO_4 (see R95). The effects of the libration motion of the PO_4 groups on the P—O bond lengths are of the order of 2% with respect to the distances obtained from the structure refinement. The **TLS**-corrected P—O distances in TlH_2PO_4 are 1.552 and 1.554 Å, rather than 1.525 and 1.528 Å, respectively, and in the case of TlD_2PO_4, the corresponding values are 1.545 and 1.556 Å, rather than 1.517 and 1.527 Å, respectively. The mean P—O distances of 1.553 (TlH_2PO_4) and 1.551 Å (TlD_2PO_4) are in close agreement.

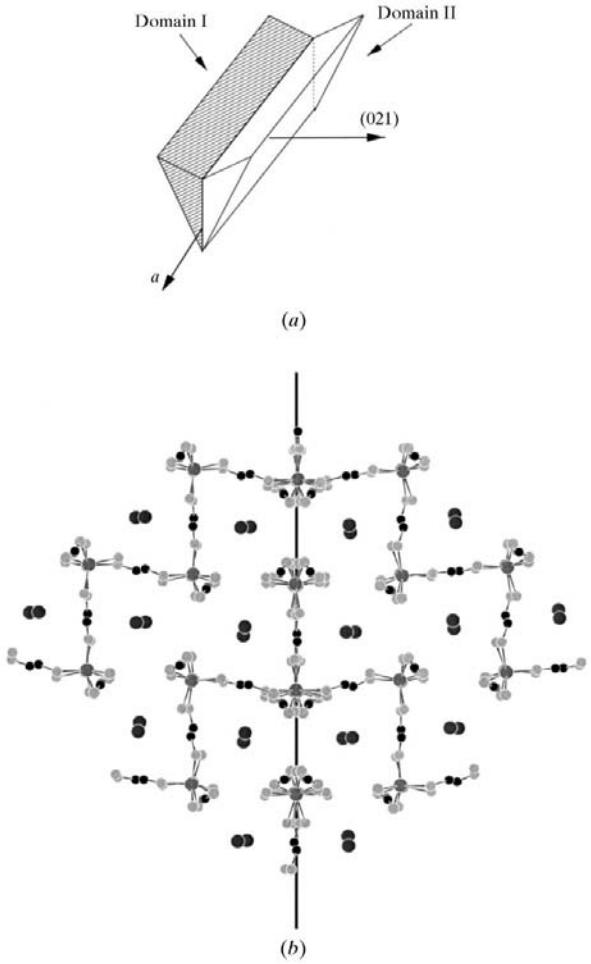

Fig. 2. (*a*) The morphology of a typical TlD_2PO_4 crystal obtained after the growing process. (*b*) View along the *a* axis of the structure of a twinned TlD_2PO_4 crystal. The twinning wall corresponds to (021) planes. Owing to the doubling of the *a* axis in the room-temperature phase, the number of atoms present in the projection is doubled.

Finally, it has to be pointed out that the anisotropy of the oxygen atomic mean-square displacement factors might also be interpreted as a consequence of the dynamical disorder related to the O—H(D)—O arrangement. In fact, the dynamical disorder of protons (deuterons) could induce a similar dynamical disorder in the PO_4 groups. Nevertheless, if this is the origin of the observed anisotropy, the distance between the two disordered positions for a given O atom would turn out to be less than 0.5 Å and thus could not be accurately analysed from the data reported in R95. Moreover, the U^{ij} parameters for P atoms and P—O distances are well defined and thus it seems that the effects of the libration motion are more important.

3. Experimental

3.1. *Samples*

The TlD_2PO_4 compound was synthesized from TlH_2PO_4 by successive exchanges with D_2O. The final deuterium concentration was higher than 98%. Colourless needle-shaped crystals of TlD_2PO_4 were obtained from a saturated solution of TlD_2PO_4 in heavy water at 340 K by a slow cooling process. Subsequent diffraction studies have demonstrated that all crystals of TlD_2PO_4 are twinned in a complex way. Two types of domains were observed. The first could be seen directly from the morphology of the crystals obtained from the growing process described above (growth twins). Fig. 2(*a*) shows a drawing of a typical TlD_2PO_4 crystal. Both twins show a common (021) plane and the *a* axis is inverted from one domain to the other. Fig. 2(*b*) shows their domain structures viewed along the *a* axis. A similar twinning type has also been seen in TlH_2PO_4 (Yoshida *et al.*, 1984). Additionally, a second type of domain was also observed. Inspection of one of the domains mentioned above revealed the simultaneous existence of two types of domain: those with the domain boundaries (100) and (or) (010), respectively. These latter domains are due to the fact that the room-temperature phase of TlD_2PO_4 is monoclinic and thus they arise from the existence of a spontaneous shear strain. Therefore, in some crystals up to eight different domains were observed. For the study reported here, a 10 mm^3 monodomain was isolated by cutting the crystal. To avoid possible deuterium $\leftrightarrow$ hydrogen exchange the crystal was protected in Al foil.

3.2. *Data collection*

Data collection was performed on the 5C.2 neutron four-circle diffractometer installed at the hot neutron beamline of the Reactor Orphée, Saclay (France). A summary of the crystal data and data collection parameters is given in Table 2.

4. Structure determination

Before directly discussing the structure determination we would like first to dedicate a few words to the controversy regarding the space group and unit cell of the room-temperature phase of TlD_2PO_4 and how this has been finally resolved. In the X-ray work of Nelmes (1981) the symmetry of the room-temperature phase of TlD_2PO_4 was reported to be monoclinic with, in analogy to the room-temperature phase of TlH_2PO_4, the *a* axis as the twofold axis. The unit cell was proposed to be *C*-centred with $2a \times 2b \times c$ as cell parameters (*a*, *b* and *c* being those of the room-temperature phase of TlH_2PO_4). Nevertheless, during the orientation of the TlD_2PO_4 crystal in our study it could be seen that, unlike in TlH_2PO_4, the *b* and *c* axes were orthogonal, while the angle between the *a* and *b* axes was not 90° (as expected), but 90.68 (5)°. This could be observed easily due to the existence of elastic domains, which provoked some of the reflections on the (*hk*0) plane to be doubled. Hence, the twofold axis of this monoclinic phase is definitely not the *a* axis, as was reported, but the *c* axis. The previous *C*-centred unit cell was transformed into a primitive unit cell by an adequate axes transformation. The new monoclinic primitive cell (mon.) is related to the prototype phase cell (ort.) by: $\mathbf{a}_{mon} = 2\mathbf{a}_{ort}$, $\mathbf{b}_{mon} = \mathbf{b}_{ort} - \mathbf{a}_{ort}$ and $\mathbf{c}_{mon} = \mathbf{c}_{ort}$, with the *c* axis as the twofold axis. Fig. 3 shows the different unit cells in the reciprocal space discussed in the text.

The diffraction pattern, therefore, shows two types of reflections: *hkl*, $h = 2n$, are associated with the reciprocal lattice of the prototype phase already studied in R95, while *hkl*, $h = 2n + 1$, are the superstructure reflections [in the reciprocal space of the prototype phase these reflections would be indexed as $(h' + \frac{1}{2}, k' + \frac{1}{2}, l)$]. According to the systematic extinctions the space group was deduced to be $P112_1/b$.† When heating the sample through the transition at 353 K and then cooling it, the splitting of $(h'k'0)$-type reflections, caused by the appearance of domains, confirmed the fact that the monoclinic axis of the room-temperature phase of TlD_2PO_4 is the *c* axis. The crystal structures of the room-temperature monoclinic phases of TlH_2PO_4 and TlD_2PO_4 are thus not isostructural.

4.1. *Refinement*

The refinement of the structure was carried out using the *CRYSTALS* program package (Watkin *et al.*, 1985). The structure was refined by a least-squares method using the atomic coordinates of the previous study of the prototype phase, R95, as starting parameters. The function minimized was $\sum w(|F_o| - |F_c|)^2$, with $w = 1/\sigma^2(F)$. Positional and anisotropic harmonic mean-square displacement parameters were refined, together with an overall scale factor. Strong reflections

† $P112_1/b$ is a non-standard setting of the space group $P12_1/c1$.

Table 2. *Experimental details*

Crystal data	
Chemical formula	TlD_2PO_4
Chemical formula weight	303.3
Cell setting	Monoclinic
Space group	$P2_1/b$
a (Å)	9.070 (6)
b (Å)	15.00 (1)
c (Å)	6.575 (5)
γ (°)	106.92 (5)
V (Å^3)	856 (1)
Z	8
D_x (Mg m^{-3})	4.51
Radiation type	Neutron
Wavelength (Å)	0.8308
No. of reflections for cell parameters	13
θ range (°)	13−22
μ (mm^{-1})	0.0015
Temperature (K)	300
Crystal form	No special shape
Crystal size (mm^3)	10
Crystal colour	Colourless
Data collection	
Diffractometer	5C.2 four-circle diffractometer
Data collection method	ω scans
Absorption correction	None
No. of measured reflections	4811
No. of independent reflections	2594
No. of observed reflections	1878
Criterion for observed reflections	$F > 3\sigma(F)$
R_{int}	0.015
θ_{max} (°)	37.33
Range of *h*, *k*, *l*	$-13 \rightarrow h \rightarrow 9$ $-21 \rightarrow k \rightarrow 21$ $-9 \rightarrow l \rightarrow 6$
No. of standard reflections	2
Frequency of standard reflections	Every 450 min
Intensity decay (%)	2
Refinement	
Refinement on	*F*
R	0.040
wR	0.038
S	1.2
No. of reflections used in refinement	1878
No. of parameters used	146
H-atom treatment	H atoms refined anisotropically
Weighting scheme	$w = 1/\sigma^2(F)$
$(\Delta/\sigma)_{max}$	0.009
$\Delta\rho_{max}$ (e Å^{-3})	0.115
$\Delta\rho_{min}$ (e Å^{-3})	−0.0903
Extinction method	Type I, Lorentzian (Larson, 1970)
Extinction coefficient	1745.1 (3)
Source of atomic scattering factors	Sears (1992)
Computer programs	
Data collection	*STADI* (Stoe, 1987)
Cell refinement	*STADI* (Stoe, 1987)
Data reduction	*STADI* (Stoe, 1987)
Structure refinement	*CRYSTALS* (Watkin *et al.*, 1985)

Table 3. *Fractional atomic coordinates and equivalent isotropic displacement parameters (Å²) for the room-temperature monoclinic phase of TlD_2PO_4*

$U_{eq} = (1/3)\Sigma_i\Sigma_j U^{ij} a^i a^j \mathbf{a}_i.\mathbf{a}_j$.

	x	y	z	U_{eq}
Tl1	0.0604 (1)	0.11848 (6)	0.2281 (2)	0.0280 (4)
Tl2	0.5631 (1)	0.13608 (6)	0.2770 (2)	0.0292 (5)
P1	0.1789 (2)	0.37445 (9)	0.2450 (3)	0.0204 (7)
P2	0.6813 (1)	0.37506 (9)	0.2526 (3)	0.0186 (7)
O11	0.2601 (2)	0.4235 (1)	0.0587 (3)	0.054 (1)
O12	0.0208 (2)	0.3048 (1)	0.1816 (3)	0.0316 (9)
O13	0.1506 (2)	0.4376 (1)	0.4085 (3)	0.0386 (9)
O14	0.2720 (2)	0.3092 (1)	0.3296 (3)	0.0287 (8)
O21	0.7901 (2)	0.4362 (1)	0.0900 (3)	0.044 (1)
O22	0.5319 (2)	0.3170 (1)	0.1626 (2)	0.0294 (8)
O23	0.6371 (2)	0.4440 (1)	0.4034 (3)	0.0356 (9)
O24	0.7735 (2)	0.3187 (1)	0.3547 (2)	0.0283 (8)
D11	0.7233 (2)	0.49093 (9)	0.4782 (2)	0.0336 (8)
D12	0.7626 (2)	0.4923 (1)	0.0275 (2)	0.0348 (8)
D21	0.3754 (1)	0.31525 (9)	0.2632 (2)	0.0324 (7)
D22	−0.0754 (2)	0.3129 (1)	0.2506 (3)	0.0349 (8)

were corrected with respect to isotropic secondary extinction. This parameter was included in the last cycles of the refinement. The final atomic parameters are listed in Table 3. Selected bond distances and angles are given in Table 4.†

5. Description of the structure of TlD_2PO_4 at 295 K

The transition of TlD_2PO_4 at T_c^d = 353 K is related to a symmetry reduction from *Pbcn* (Z = 4) to $P112_1/b$ (Z = 8), with the c axis of the prototype phase as the unique twofold axis of the room-temperature phase. From the group-to-subgroup relation, the order parameter is known to have S_1^+ symmetry with the wavevector $\mathbf{q}$ = ($\frac{1}{2}$,$\frac{1}{2}$,0). Fig. 4 shows the structure of TlD_2PO_4 at 295 K in a projection along [001] referring to the monoclinic cell (the prototype-phase cell is indicated by dotted lines). This phase is characterized by the complete ordering of both types of D atoms, D1 and D2. The new O—D distances are now close to 1.0 Å; more specifically, the average length is 1.016 (2) Å. In the deuteron-ordering process one of the two crystallographic centres of inversion (the one in which D1-type atoms are situated) is lost. The dynamical disorder of D atoms in the prototype phase is known to be directly correlated to the configuration of the PO_4 groups. Therefore, in the room-temperature phase, the freezing of D atoms in one of the two off-centre positions is accompanied by a strong distortion of the PO_4 groups. This distortion may be noticed from the new P—O bond distances and O—P—O angles listed in Table 4. In Fig. 4, long P—O bonds are indicated by dotted lines and short ones by solid lines. At the transition, while inside a given chain parallel to the c axis two given D1-type atoms move towards a given PO_4 group, in the next neighbouring chain in the [100] direction these atoms move in the opposite direction. The projection of this motion in the ab plane is indicated in Fig. 4 by the small arrows close to each of the D1-type atoms. The dipole moments induced in the PO_4 tetrahedra due to their internal distortion (*i.e.* the relative displacement of P atoms with respect to the surrounding O atoms) lie along the b axis and the doubling of the cell parameter in the a direction leads to the antiferroelectric nature of this phase.

† Supplementary data for this paper are available from the IUCr electronic archives (Reference: LC0004). Services for accessing these data are described at the back of the journal.

6. Discussion

6.1. *Transition at T_I in TlH_2PO_4*

It has already been pointed out that in TlH_2PO_4 the transition at T_I is of a ferroelastic type: from the orthorhombic space group *Pbcn* to the monoclinic $P2_1/b11$. In this case, from a group-to-subgroup analysis the symmetry of the order parameter is deduced to be B_{3g} (at q = 0). In order to determine the atomic and molecular motions involved in this phase transition, the individual atomic displacements in the room-temperature phase with respect to the prototype phase were analysed. The atomic displacements of Tl and H2 atoms (H1 still disordered) were observed to be rather small (<0.05 Å). To analyse the atomic displacements of PO_4 groups, the displacement field was fitted to a rigid-body model, as described below. The function minimized was $\sum(d_o - d_c)^2$, where d_o are the observed and d_c the calculated atomic displacements in a rigid-body approximation (*i.e.* as a combination of rotational and translational movements). The agreement factor for the best fit corresponds to the value $[\sum(d_o - d_c)^2 / \sum d_o^2]^{1/2} = 0.12$ and the result obtained is: R_x = −6.8, R_y = −0.1, R_z = 0.3 and T_x = −0.023, T_y =

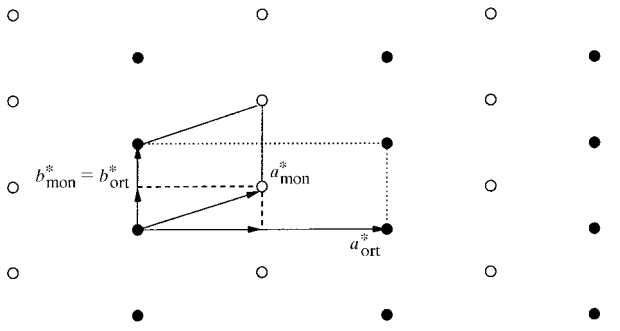

Fig. 3. (*hk*0) plane of the reciprocal lattice of the room-temperature phase of TlD_2PO_4. (•) and (○) indicate basic and superstructure reflections, respectively. The prototype-phase cell (dotted lines), the unit cell proposed by Nelmes (1981) (dashed lines), with the a axis as the twofold axis, and the unit cell proposed in our study (solid lines), with the c axis as the twofold axis, are also indicated.

Table 4. *Selected geometric parameters (Å, °) for TlD_2PO_4*

P1—O11	1.505 (3)	O21—D12	1.027 (3)
P1—O12	1.567 (2)	D12—O11^{i}	1.458 (2)
P1—O13	1.503 (3)	O12—D22	1.018 (2)
P1—O14	1.569 (2)	D22^{ii}—O24	1.561 (2)
P2—O21	1.559 (3)	O23—D11	1.009 (3)
P2—O22	1.501 (2)	D11—O13^{iii}	1.520 (3)
P2—O23	1.568 (2)	O14—D21	1.012 (2)
P2—O24	1.508 (2)	D21—O22	1.563 (2)
O11—P1—O12	109.3 (2)	O21—P2—O22	112.5 (2)
O11—P1—O13	115.2 (2)	O21—P2—O23	106.4 (1)
O11—P1—O14	108.5 (1)	O21—P2—O24	106.0 (1)
O12—P1—O13	108.7 (1)	O22—P2—O23	105.8 (1)
O12—P1—O14	103.3 (1)	O22—P2—O24	113.9 (1)
O13—P1—O14	111.2 (2)	O23—P2—O24	112.2 (2)

Symmetry codes: (i) $1-x, 1-y, -z$; (ii) $1+x, y, z$; (iii) $1-x, 1-y, 1-z$.

0.0006, $T_z = -0.012$, where R indicates the rotation part and T the translation part, expressed in ° and relative units, respectively. From these results it can be seen that the displacement field of the PO_4 groups corresponds to a rotation of the rigid body around the *a* axis. The good agreement between calculated and observed displacements indicates that the PO_4 groups in the room-temperature phase are only slightly distorted with respect to the almost perfect configuration in the prototype phase. From a symmetry mode analysis (*e.g.* Pérez-Mato *et al.*, 1986) it can be seen that the only atomic displacements contributing to the observed ferroelastic distortion will correspond to modes transforming according to the irreducible representations of the space group *Pbcn*, labelled B_{3g} and A_{1g} with $q = 0$. The modes of B_{3g} symmetry are polarized along the *x* and *z* directions, and A_{1g} modes along the *y* direction. Therefore, the displacement field of PO_4 groups observed in our case (which is mainly along the *x* direction) would correspond to the freezing, at the transition, of a libration optic mode of B_{3g} symmetry and eigenvector along the *a* axis. This optic mode is expected to be coupled linearly to the spontaneous shear strain (of B_{3g} symmetry) and trigger the ferroelastic transition observed in TlH_2PO_4 at T_I. Moreover, the amplitude at room temperature of the frozen rotation found above is in reasonably good agreement with the amplitude of the libration movement estimated at 373 K in the prototype phase from the **TLS** analysis. A Raman-scattering study of the low-frequency modes of TlH_2PO_4 would be necessary to confirm the existence of such a soft librational mode at 357 K.

6.2. *H/D bonds*

With regard to the H atoms, in the ferroelastic phase of TlH_2PO_4 they are partially ordered: H1-type atoms are still dynamically disordered, while H2-type atoms become ordered. In the case of H1 atoms this can be seen from the structural data, *i.e.* they are still situated in a special position and the O—H1 bond length is ~1.2 Å, as well as from NQR measurements (Seliger *et al.*, 1988), where H1 atoms are shown to order at the antiferroelectric transition at 230 K. In the case of H2, however, it should be stressed that the O—H2 bond length at room temperature is slightly longer [1.15 (2) Å] than the typical O—H distance of ~1 Å. This result might be explained if H2-type atoms are supposed to become completely 'attached' to the O atom in a continuous way, as the rotation of PO_4 groups reaches its saturation value. To confirm this hypothesis new diffraction measurements would be required in the range from room temperature to 230 K. H2 hydrogen bonds do not seem to play a significant role in this transition.

As already mentioned, H1-type atoms do become ordered only after having undergone the transition at 230 K. Although there is no direct evidence for the antiferroelectric nature of this low-temperature phase in TlH_2PO_4, the similarity of the behaviour of the dielectric constant along the *a* axis *versus* temperature with that observed in antiferroelectric $NH_4H_2PO_4$ and TlD_2PO_4 (Yasuda, Fujimoto, Asano *et al.*, 1980) suggests that the low-temperature phase of TlH_2PO_4 is also antiferroelectric. Thus, it seems that in both compounds, TlH_2PO_4 and TlD_2PO_4, antiferroelectricity is directly associated with the ordering of H1 (D1)-type atoms. Thus, H2 atoms do not play a relevant role in the structural phase transitions described; they seem simply to follow the motion of the PO_4 groups. In fact, one may wonder whether H2 (D2)-type atoms are really disordered in a double well potential in the prototype phase,

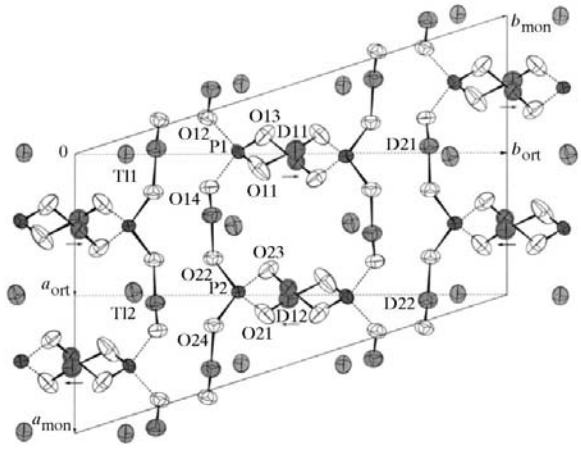

Fig. 4. Projection along the [001] direction of the structure of the room-temperature monoclinic phase of TlD_2PO_4. The relation between the prototype-phase cell (dotted line) and the monoclinic phase cell (solid line) is shown. Small arrows indicate the direction in which the D1-type atoms approach a given tetrahedron. The distortion of the tetrahedra is shown by indicating the short P—O bond lengths as solid lines and the long bond lengths as dotted lines.

as H1 (D1)-type atoms, or if the potential shape looks more like an anharmonic single potential. In this case their motion would be less critical regarding the transitions described in this paper.

Finally, we would like to stress that the critical antiferroelectric fluctuations in TlH_2PO_4 and TlD_2PO_4 seem to occur inside the O—H1(D1)—O arrangements. These compounds may be thus considered as one-dimensional systems from the point of view of the proton/deuteron ordering, as in *e.g.* CsH_2PO_4. Nevertheless, we should remind the reader that in this latter compound deuteration does not seem to induce such important effects as those observed in the TlH_2PO_4/TlD_2PO_4 system with respect to their two different phase transition sequences.

6.3. *Low-temperature phases*

The vibrational study undertaken of the low-temperature phase of both compounds ($T < 230$ K for TlH_2PO_4 and $T < 127$ K for TlD_2PO_4) by means of Raman spectroscopy on powder samples (Pasquier *et al.*, 1993) seems to evidence an analogy between the spectra and thus the possibility that these two compounds are structurally isomorphous at low temperatures.

Owing to the difficulty of obtaining single crystals of TlD_2PO_4 (these are expected to twin below the transition at 127 K), a preliminary powder neutron diffraction study (working with $\lambda = 4.75$ Å) has been carried out over the temperature range 200–80 K in order to investigate the symmetry change at the transition. Unfortunately, owing to the low symmetries involved in this transition and thus the large number of Bragg reflections present in the diagram, analysis of the symmetry change was not obvious. Nevertheless, when looking at the 021 and 041 reflections of the monoclinic phase (the only ones which do not overlap in the 2θ range studied, 10–150°), the behaviour with temperature of both the FWHM (full width at half-maximum) and the intensity evidences the fact that they split at the transition. Fig. 5 shows (*a*) the FWHM and (*b*) the intensity of these two Bragg reflections as a function of the temperature.

Fig. 5(*a*) shows the almost constant behaviour of the FWHM above the transition and how it increases rapidly below the transition. This originates from the fact that above the transition these reflections are single peaks and only slightly temperature-dependent, while below (although not directly visible) the reflections split into two peaks ($02\bar{1}$ and 021, and $04\bar{1}$ and 041, respectively). The intensity (Fig. 5*b*) increases slowly upon lowering the temperature, as expected from a decrease in the thermal vibration. At the transition, however, there is a

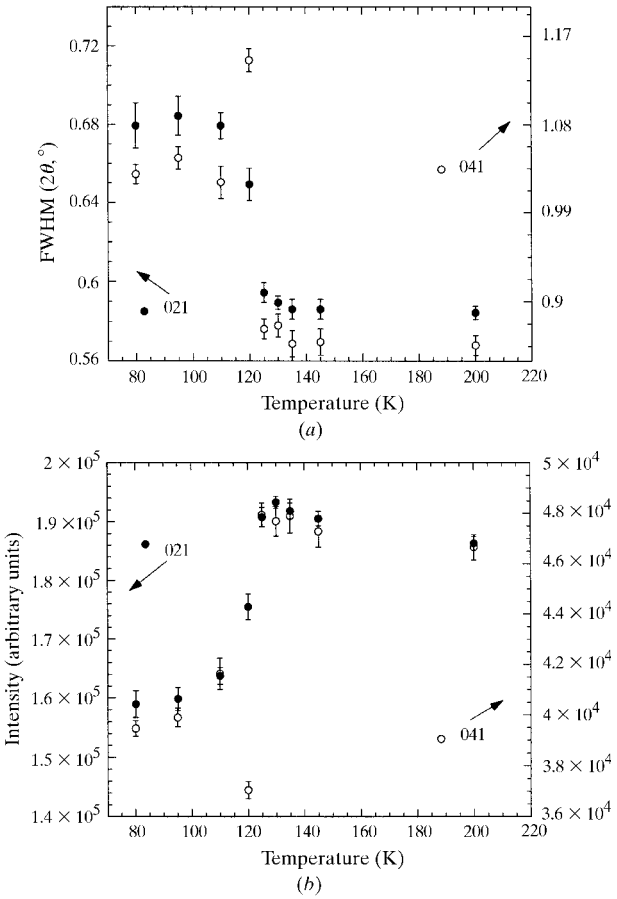

Fig. 5. (*a*) The FWHM and (*b*) the intensity of the two Bragg reflections 021 and 041 as a function of temperature for TlD_2PO_4. Both, the FWHM and the intensity were obtained from fitting the data to one Gaussian function. The measurements were carried out at decreasing temperature.

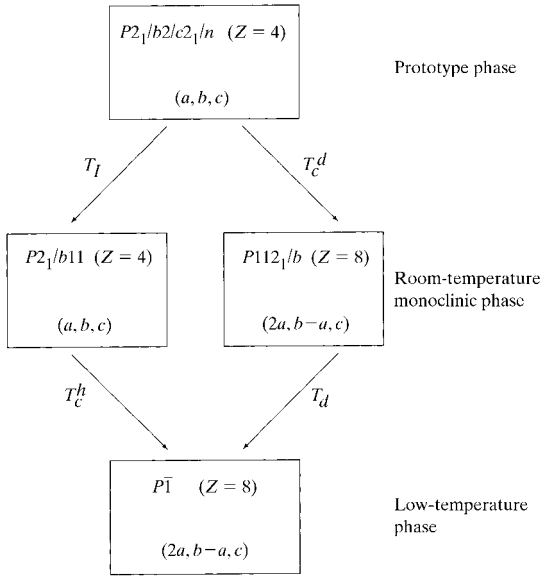

Fig. 6. Scheme of the phase sequence shown by TlH_2PO_4 and TlD_2PO_4 on decreasing the temperature.

large decay that should be attributed to the splitting of the reflections. It may be noticed that the behaviour of both reflections with respect to temperature is rather similar, although the discontinuity at the transition is more pronounced at high scattering angles, *i.e.* for the 041 reflection. Our results thus seem to reveal that for TlD_2PO_4, and below 127 K, the symmetry is reduced from monoclinic to triclinic. Further studies are in progress to determine more specifically the structural changes involved in this transition. Finally, it should be pointed out that the transition temperature derived from our measurements (between 120 and 125 K) does not exactly correspond to that reported in the literature (127 K). This shift probably originates from the uncertainty in the measurement of the temperature.

From recent X-ray diffraction measurements on TlH_2PO_4 at 210 K (Heger *et al.*, 1995), the structure of this phase is known to have triclinic symmetry also, with space group $\bar{1}$. Therefore, at low temperatures, when all H (D) atoms are ordered, both compounds effectively seem to be isostructural. The phase sequences observed in TlH_2PO_4 and TlD_2PO_4 may thus be summarized schematically as shown in Fig. 6.

7. Conclusions

Our structural study of the different phases of TlH_2PO_4 and the fully deuterated form TlD_2PO_4 has revealed the two different sequences they exhibit as a function of the temperature. Up to now this compound is the only one of this family of materials to show such a variation of its phase sequence with deuteration. It is known that highly deuterated compounds differ structurally from their protonated homologues [*e.g.* Thornley *et al.* (1975) have shown that $K(H_{1-x}D_x)PO_4$ is tetragonal at room temperature for $x < 0.99$ and monoclinic for $x > 0.99$], but to our knowledge no further studies have been carried out in this direction to clarify the effects of high degrees of deuteration in relation to their phase diagram.

It would be interesting to proceed further and carry out a detailed study of the mixed compounds $Tl(H_xD_{1-x})_2PO_4$, with $0 < x < 1$, to determine their phase sequence and to see over which critical degree of deuteration do these compounds show the same behaviour as the highly deuterated compound.

One of us (SR) acknowledges the Research Department of the Government of the Basque Country for financial support. We express our thanks to B. Pasquier and N. Le Calvé for providing the samples of TlD_2PO_4 and J. M. Godard for growing the crystals. We would also like to thank I. Etxebarria for helpful discussions.

References

Arai, M., Yagi, T., Sakai, A., Komukae, M., Osaka, T. & Makita, Y. (1990). *J. Phys. Soc. Jpn*, **59**, 1285–1292.

Bousquet, J., Diot, M., Tranquard, A., Coffy, G. & Vignalou, J. R. (1978). *J. Chem. Thermodyn.* **10**, 779–786.

Hanazawa, K., Komukae, M., Osaka, T., Makita, Y., Arai, M., Yagi, T. & Sakai, A. (1991). *J. Phys. Soc. Jpn*, **60**, 188–195.

Heger, G., Glinnemann, J. & Becker, M. (1995). Private communication.

Hirshfeld, F. L. (1976). *Acta Cryst.* A**32**, 239–244.

Larson, A. C. (1970). *Crystallographic Computing*, edited by F. R. Ahmed, S. R. Hall & C. P. Huber, pp. 291–294. Copenhagen: Munksgaard.

Matsuo, T. & Suga, H. (1977). *Solid State Commun.* **21**, 923–927.

Narasaiah, T. V., Choudhary, R. N. P., Nigam, G. D. & Mattern, G. (1986). *Z. Kristallogr.* **175**, 145–149.

Nelmes, R. J. (1981). *Solid State Commun.* **39**, 741–743.

Nelmes, R. J. & Choudhary, R. N. P. (1981). *Solid State Commun.* **38**, 321–324.

Nelmes, R. J., Meyer, G. M. & Tiballs, J. E. (1982). *J. Phys. C*, **15**, 59–75.

Oddon, Y., Tranquard, A. & Pépe, G. (1979). *Acta Cryst.* B**35**, 542–546.

Oddon, Y., Vignalou, J. R., Coffy, G. & Tranquard, A. (1976). *Bull. Soc. Chim.* **3–4**, 334–336.

Pasquier, B., Le Calvé, N., Al-Homsi-Teiar, S. & Fillaux, F. (1993). *Chem. Phys.* **171**, 203–220.

Pérez-Mato, J. M., Gaztelua, F., Madariaga, G. & Tello, M. J. (1986). *J. Phys. C*, **19**, 1923–1935.

Ríos, S., Paulus, W., Cousson, A., Quilichini, M., Heger, G., Le Calvé, N. & Pasquier, B. (1995). *J. Phys. Fr.* **5**, 763–769.

Schomaker, V. & Trueblood, K. N. (1968). *Acta Cryst.* B**24**, 63–76.

Sears, V. F. (1992). *Neutron News*, **3**, 26–37.

Seliger, J., Zagar, V., Blinc, R. & Schmidt, V. H. (1988). *J. Chem. Phys.* **88**, 3260–3262.

Stoe (1987). *STADI*. Stoe & Cie, Darmstadt, Germany.

Thornley, F. R., Nelmes, R. J. & Rouse, K. D. (1975). *Chem. Phys. Lett.* **34**, 175–177.

Tun, Z., Nelmes, R. J., Kuhs, W. F. & Stansfield, R. F. D. (1988). *J. Phys. C*, **21**, 245–258.

Watkin, D. J., Carruthers, J. R. & Betteridge, P. W. (1985). *CRYSTALS User Guide*. Chemical Crystallography Laboratory, University of Oxford, England.

Yasuda, N., Fujimoto, S. & Asano, T. (1980). *Phys. Lett. A*, **76**, 174–176.

Yasuda, N., Fujimoto, S., Asano, T., Yoshino, K. & Inuishi, Y. (1980). *J. Phys. D*, **13**, 85–94.

Yoshida, H., Endo, M., Kaneko, T., Osaka, T. & Makita, Y. (1984). *J. Phys. Soc. Jpn*, **53**, 910–912.